

Ram Accelerator Operating Limits, Part 2: Nature of Observed Limits

A. J. Higgins,* C. Knowlen,† and A. P. Bruckner‡
University of Washington, Seattle, Washington 98195

The causes of unstarts, which limit the operation of ram accelerators, are investigated. Prior experiments have identified distinct limits as functions of the projectile Mach number and the energy content of the propellant mixture. When a ram accelerator projectile enters a very energetic mixture, a normal shock is immediately driven in front of it. The mechanism of this unstart was examined by stripping the driving combustion wave from the projectile before it entered the test mixture. The projectile in this case was able to coast supersonically without unstart, which suggests the unstart mechanism is a surge of the driving combustion wave past the projectile throat. In less energetic mixtures, projectiles are able to accelerate beyond the detonation speed of the mixture before unstating. This unstart mechanism was investigated by changing the projectile material from Mg to Al and from Al to Ti, which allowed the projectile to accelerate to even higher Mach numbers. These results show the unstart mechanism in these cases to be a projectile structural effect, not a gasdynamic phenomenon. An experiment with an all-Ti projectile was able to withstand the intense heat transfer environment in the ram accelerator.

Introduction

RECENT research on the ram accelerator concept^{1,2} at the University of Washington (UW) has focused on the limits of operation of the thermally choked ram accelerator.^{3–6} This work is summarized in Ref. 7. While the range of propellant chemistry and projectile Mach number that will sustain successful ram acceleration has been experimentally determined, the phenomena that limit operation, particularly “unstarts” in which a normal shock wave is driven in front of the projectile, are not completely understood. For example, in prior experiments in which the projectile has traveled several meters before unstating, it has proven difficult to differentiate an unstart caused by gasdynamic and combustion phenomena from an unstart caused by a structural failure of the projectile. This paper reports an investigation into the nature of the mechanisms, both gasdynamic and structural, which limit operation of the thermally choked ram accelerator.

A one-dimensional flowfield model predicts the operational range of the ram accelerator, which can be shown on a plot of nondimensional heat release $Q = \Delta q/c_{p1} T_1$ and Mach number.⁷ Figure 1 shows the theoretical envelope of operation for a projectile with an annular throat-to-tube area ratio of 0.42 and an annular base-to-tube area ratio of 0.76, which corresponds to the nominal UW projectile geometry. In Fig. 1 the dashed line shows the Chapman–Jouguet (CJ) detonation Mach number as a function of Q .

The applicability of this flowfield model has been experimentally investigated by determining the region of ram accelerator operation as a function of the projectile Mach number and mixture heat release.⁷ By varying the amount of nitrogen dilution in a $2.8\text{CH}_4 + 2\text{O}_2 + \text{XN}_2$ class of propellant mixture

at 25-atm fill pressure, the limits to ram acceleration have been identified for Mg alloy projectiles. These experimental limits to operation are labeled “a” to “d” in Fig. 1. Similar limits have been identified for Al projectiles in a $2\text{H}_2 + 2\text{O}_2 + \text{XCH}_4$ class of mixture at 50-atm fill pressure.⁷ The experimentally determined envelopes of operation are seen to occupy a different region of the heat release–Mach number (Q – M) plane than suggested by the one-dimensional model of the flowfield. The ram accelerator can operate at Mach numbers where an ideal normal shock would have fallen off the projectile. In fact, the projectile can continue to accelerate beyond the CJ detonation speed of the mixture, which the one-dimensional thermally choked model predicts as the maximum speed obtainable in a given mixture.¹ It appears to be unable, however, to access the higher values of heat release that the one-dimensional model indicates should support ram accelerator operation.

The experimentally determined region of operation in Fig. 1 is bounded by four distinct limits.⁷ The first, labeled “a,” is an immediate unstart that occurs when projectiles enter mixtures with too great a heat release. The “b” limit is also composed of unstarts that occur after the projectiles have been accelerated for at least 1 m. Experiments in more diluted mixtures with lower values of heat release allow the projectile to travel at least 10 m into the test section and exhibit “trans-detonative” operation. These experiments, however, are also terminated by unstarts, which form the “c” limit in Fig. 1. Finally, the “d” limit is the only observed operational limit that is not the result of an unstart. Instead, it corresponds to a quenching of the combustion process and a fall-off of the driving normal shock system from the projectile afterbody. Because the usual interest is in increasing the heat release of a mixture or the Mach-number range of the projectile, no further attention is paid to the d limit, which is a minimum requirement on the mixture heat release.

This paper presents an investigation of the mechanisms that comprise these limits to ram accelerator operation. The cause of the gasdynamic unstart mechanism was explored by intentionally stripping the combustion wave from the projectile and then injecting the coasting projectile back into the combustible test mixture. The suspected structural unstart mechanism was investigated by selectively altering the material from which parts of the projectiles were fabricated.

Received Jan. 10, 1997; revision received Feb. 5, 1998; accepted for publication April 5, 1998. Copyright © 1998 by the authors. Published by the American Institute of Aeronautics and Astronautics, Inc., with permission.

*Graduate Research Assistant, Department of Aeronautics and Astronautics; currently Postdoctoral Research Fellow, Department of Mechanical Engineering, McGill University, Montreal, Quebec H3A 2K6, Canada. Member AIAA.

†Research Scientist, Department of Aeronautics and Astronautics. Senior Member AIAA.

‡Professor and Chair, Department of Aeronautics and Astronautics. Fellow AIAA.

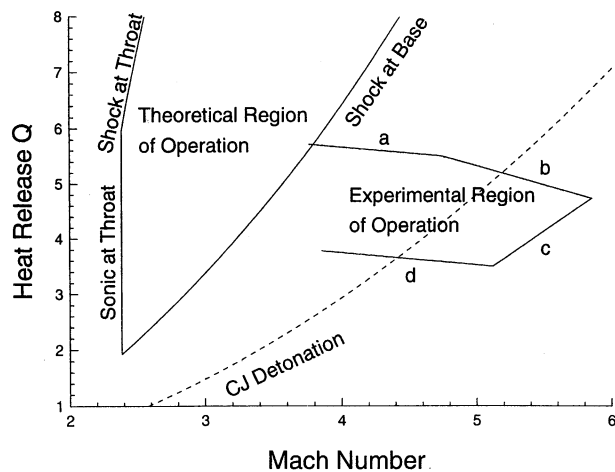


Fig. 1 Theoretical and experimental envelopes of ram accelerator operation, shown as mixture heat release ($Q = \Delta q/c_p T_1$) vs projectile Mach number.

Gasdynamic Limits

Unstart Mechanisms

A one-dimensional model that treats the flow past the projectile as isentropic, except for a single normal shock stabilized by combustion occurring behind the projectile, suggests two possible unstart mechanisms.⁷ First, if the projectile is traveling below the minimum Mach number required to maintain supersonic flow past the projectile throat, the flow will choke on the projectile forebody, causing an unstart. Second, if the heat release of combustion is too great the normal shock will be driven over the projectile throat, also resulting in an unstart. These unstart mechanisms are represented schematically in Fig. 2 and their Q - M relations are labeled "sonic at throat" and "shock at throat," respectively, in Fig. 1. Although they appear relevant only at Mach numbers less than Mach 3, the effect of precombustion, which becomes more pronounced as the mixture heat release is increased by reducing the amount of dilution, can make these mechanisms significant at much higher Mach numbers. For example, precombustion on the projectile forebody has the effect of driving the flow to sonic, making choking of the flow at the throat more likely. It also has the effect of moving the ideal normal shock forward, making the shock at throat mechanism more likely as well. Thus, either of these two mechanisms may be responsible for the observed gasdynamic unstarts comprising the a and b limits of Fig. 1.

More detailed models of the ram accelerator flowfield suggest several possible mechanisms of precombustion unstarts initiated by the conical shock wave, particularly in superdetonative operation, where the projectile is traveling faster than the CJ detonation speed. Ghorbanian et al.⁸ analyzed the amount of propellant that will be combusted in the stagnation zone at the projectile nose tip that has been blunted by the hypersonic environment. Lefebvre and Fujiwara⁹ computationally simulated the initiation of forward-propagating detonations by conical blunt bodies. Leblanc et al.¹⁰ performed computational fluid dynamics (CFD) simulations of the flow over the projectile forebody of a superdetonative ram accelerator and observed instances of detonation developing where the oblique shocks reflect between the tube wall and throat and then propagate ahead of the projectile. Ghorbanian and Sterling¹¹ suggested a superdetonative unstart mechanism in which the oblique shock from the nose cone reflects as a normal detonation Mach stem or as a strong oblique detonation at the tube wall. Messersmith and Reeb¹² also discussed unstarts resulting from the Mach reflection of the initial shock as a normal detonation. All of these analytical and computational investigations suggest unstart mechanisms that are independent

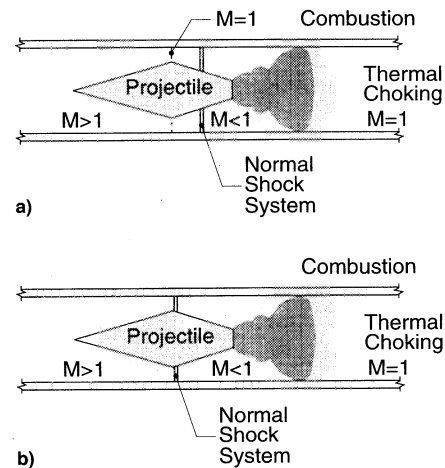


Fig. 2 Two mechanisms of unstart predicted by one-dimensional modeling: a) sonic at throat and b) shock at throat.

of the flowfield behind the projectile, thus it is unclear whether any of these phenomena could be responsible for the unstarts that limit the thermally choked and transdetonative operation examined in this study.

Other computational simulations have examined how the combustion behind the projectile can propagate over the throat, resulting in an unstart. Simulations performed by Soetrismo et al.¹³ showed that boundary-layer combustion and the oblique shock system (in transdetonative operation there is no longer a normal shock) can move up the projectile body and approach the throat. These simulations are particularly noteworthy in that they used the same chemistry and projectile geometry as the UW ram accelerator. Superdetonative simulations performed by Yungster¹⁴ also identified boundary-layer combustion and separation as a way for combustion to propagate forward from behind the projectile and cause an unstart. Nusca¹⁵ observed the forward propagation of boundary-layer combustion and combustion at the projectile nose tip leading to unstart in a CFD simulation of a 120-mm bore ram accelerator projectile as it accelerated through the transdetonative regime.

All of these possible phenomena can be divided into the two classes of unstart as suggested by the one-dimensional model in Fig. 2: a) Unstarts resulting from choking the flow over the projectile forebody and b) unstarts resulting from the normal shock wave propagating from behind the projectile past the throat. The distinction between these two classes is not mere terminology because the remedy for the unstart problem is different in either case. According to the one-dimensional model of the flowfield, decreasing the throat diameter of the projectile (thus increasing the flow area there) should prevent choking unstarts on the forebody. Alternatively, increasing the throat diameter should allow the projectile to better contain a normal shock system behind the throat.⁷

Because the flow over the projectile forebody is supersonic, the first unstart mechanism is independent of the combustion wave stabilized behind the projectile, whereas the second unstart mechanism requires the combustion wave. This difference suggests a way to experimentally identify which of these two mechanisms is responsible for the observed limits. Because a complex and unsteady interaction with the obturator used in launching the projectile from the gas gun prelauncher initiates the driving combustion wave,^{16,17} the operation of the projectile without the presence of the combustion wave can be examined by first "stripping" combustion from the projectile. By passing the projectile through a section of tube filled with inert gas, the projectile can be injected into a mixture that has been previously identified as being too energetic to support operation. If the projectile then immediately unstarts, the unstart mechanism does not require the presence of the combustion wave behind the projectile and is most likely some form of precombustion

leading to thermal choking at the projectile throat. If the projectile does not unstart, and simply coasts supersonically through the tube uneventfully, the unstart mechanism then requires that the combustion wave first be established behind the projectile and is not purely a result of the flow past the projectile forebody. This type of experiment was used to investigate the cause of unstarts in the $2.8\text{CH}_4 + 2\text{O}_2 + \text{XN}_2$ and $2\text{H}_2 + 2\text{O}_2 + \text{XCH}_4$ classes of propellant. The experiment details and results are discussed next.

Experimental Procedure

The projectiles, experimental facility, and procedure used in these experiments are identical to those discussed in Ref. 7. The only difference between prior experiments (Fig. 3a), which mapped the operating limits to ram acceleration, and the present experiments (Fig. 3b), which examined the ability

of the projectile to coast supersonically through a given propellant, is the addition of a stage of inert gas between the initial starter stage and the test mixture.

The inert stage used to strip the combustion wave from the projectile was selected to be as similar to the test mixture as possible. For the $2.8\text{CH}_4 + 2\text{O}_2 + \text{XN}_2$ class of propellant, the O_2 was simply replaced with additional N_2 . For example, if the test mixture was $2.8\text{CH}_4 + 2\text{O}_2 + 3\text{N}_2$, the combustion stripping was performed with $2.8\text{CH}_4 + 5\text{N}_2$. For the $2\text{H}_2 + 2\text{O}_2 + \text{XCH}_4$ class of propellant, the mixture thermodynamic properties are almost independent of the methane content, and so the combustion stripping was effected with a section of pure methane. The use of an inert gas with nearly the same acoustic impedance as the test gas assures a smooth transition without complex wave reflections at the mixture interface.

Results

For the $2.8\text{CH}_4 + 2\text{O}_2 + \text{XN}_2$ class of propellant at 25 atm, whose experimentally determined operational envelope is shown in Fig. 1, the minimum amount of N_2 dilution that would allow operation was 3.7N_2 .⁷ This mixture forms the a limit depicted in Fig. 1. Mixtures with higher values of heat release, i.e., with N_2 dilution reduced to 3.0N_2 or 3.4N_2 , caused the projectile to immediately unstart upon transition from the starter stage to the test mixture. A series of pressure traces from such an experiment with the projectile transitioning to a test mixture of $2.8\text{CH}_4 + 2\text{O}_2 + 3.0\text{N}_2$ at 1360 m/s (Mach 3.7) is shown in Fig. 4a. These traces are taken from wall-mounted pressure transducers located at 40-cm intervals along the ram accelerator tube. The pressure traces are synchronized with the passage of the projectile throat at $t = 0$. The projectile length

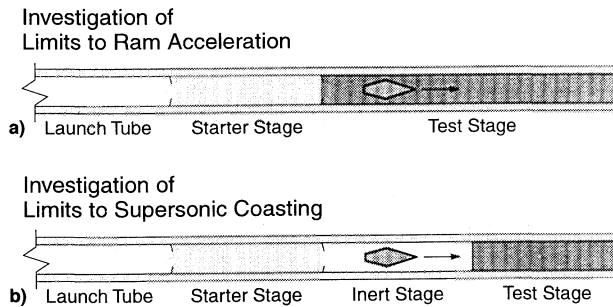


Fig. 3 Experimental configurations used in investigating a) limits to ram acceleration and b) supersonic coasting without the driving combustion wave.

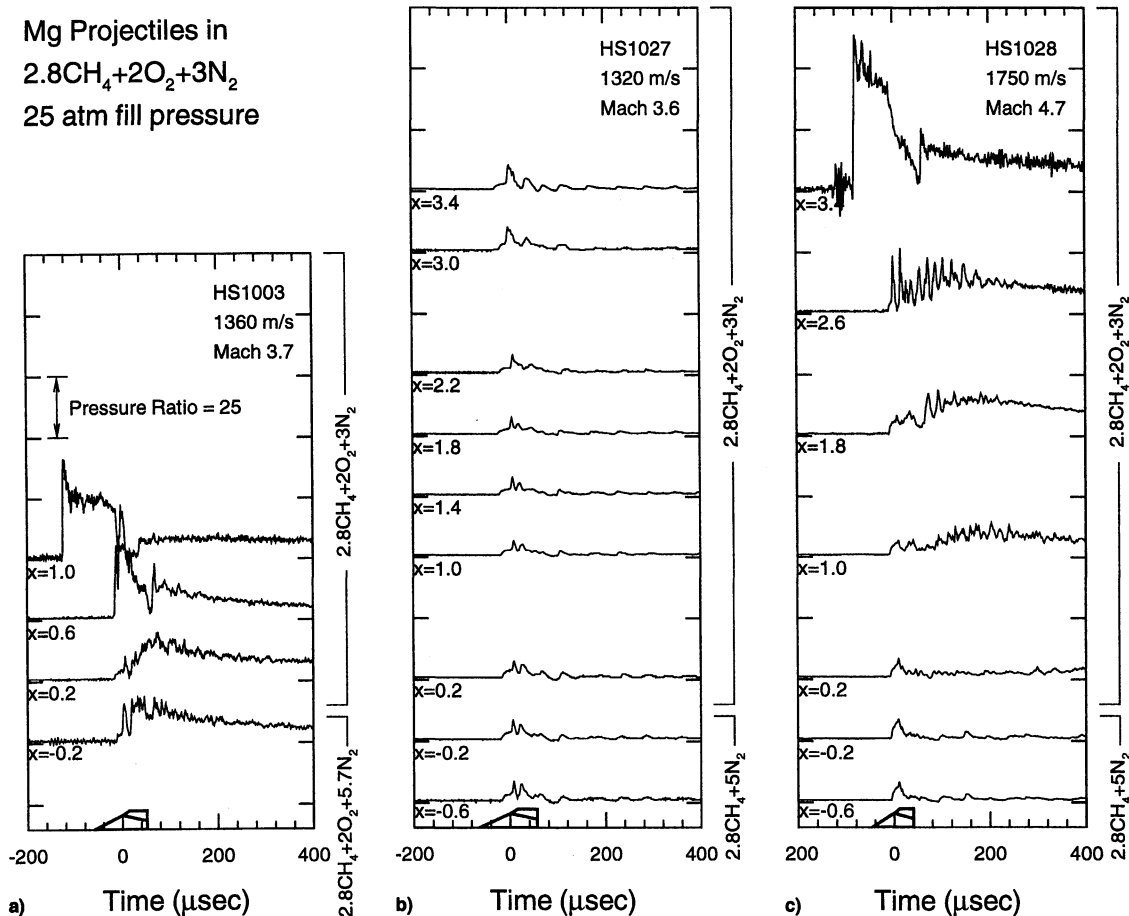


Fig. 4 Pressure traces from a mixture with a heat release value too great to support ram accelerator operation: a) projectile enters test mixture with combustion wave attached; b) projectile enters from inert stage without combustion wave attached; and c) projectile enters test mixture from inert stage at higher Mach number.

is shown relative to the time scale of the data. The location of each transducer relative to the diaphragm at the entrance of the test section is given. For example, " $x = 0.2$ " indicates a pressure trace from a transducer located 0.2 m past the diaphragm at the entrance to the test section. The first trace, labeled " $x = -0.2$ " in Fig. 4a, is taken from the starter stage and is typical of nominal ram accelerator operation.^{2,18} As the projectile entered the test mixture, a strong shock wave formed at the throat and quickly propagated in front of the projectile after less than 1 m of travel, indicating an unstart that in this case developed into a detonation.

To determine the cause of this unstart, the experiment in Fig. 4a was repeated, only now the projectile passed through an inert stage before entering the test mixture of $2.8\text{CH}_4 + 2\text{O}_2 + 3\text{N}_2$. The projectile Mach number was slightly lower (Mach 3.6 instead of Mach 3.7). It should be noted that no ram acceleration was involved in this particular experiment; the gas gun prelauncher was able to accelerate the projectile to the desired test velocity before it entered the inert stage. The result of the experiment is shown as a series of pressure traces in Fig. 4b. The first two traces shown are from the inert stage of $2.8\text{CH}_4 + 5\text{N}_2$ and are typical profiles for a projectile coasting supersonically in a nonreacting mixture.¹⁹ Conical shocks are still visible reflecting from the tube wall near the projectile throat, but no high-pressure combustion wave is visible behind the projectile. When the projectile entered the combustible mixture, no change in the pressure field around the projectile occurred. The projectile proceeded supersonically down the tube, gradually decelerating as a result of aerodynamic drag, but without unstarting. This result demonstrates that the flow past the projectile throat can remain supersonic if the combustion wave is first stripped or not allowed to form, while a projectile entering the same mixture with the combustion wave attached immediately unstarts. This combustion-stripping experiment is represented as a triangle labeled "1" in Fig. 5. Here, the value of Q for thermally choked operation has been ascribed to the mixture, even though no combustion was observed.

As the projectile velocity at transition to the test mixture was increased, a different result was observed. Figure 4c shows a series of pressure traces for a projectile that transitioned to the test mixture from the inert stage at Mach 4.7. At 1.0 m after transition, a wave is seen developing in the wake of the projectile and growing in amplitude as it overtakes the projectile. While the projectile was between $x = 1.0$ and 2.6 m into the test section, this combustion wave was exerting thrust because the projectile was observed to accelerate from 1750 to 1810 m/s. Thus, ram accelerator drive had been transiently reestablished in this experiment. However, the combustion wave could not be contained on the projectile, and by 3 m into the test section it had surged past the throat, resulting in an unstart. Until this time, however, the pressure profile at the projectile throat remained unchanged in character and amplitude. Thus, the unstart mechanism in this mixture is not associated with precombustion on the projectile forebody, but instead is observed to be a surge of the combustion driven shock system past the projectile. Because the projectile coasted over 2 m without unstart, this experiment is also labeled as successful supersonic coast "3" in Fig. 5. Transition from inert gas to the test mixture at Mach 4.2 generated a similar result and is labeled "2" in Fig. 5. The fact that the projectile was able to coast for at least 2 m without unstart in mixtures significantly more energetic than the gasdynamic limit to operation in all three of the combustion stripping experiments shown in Fig. 5 is strong evidence that the unstart mechanism requires the presence of combustion behind the projectile.

This technique of diagnosing unstarts was also performed on the operational limits to the $2\text{H}_2 + 2\text{O}_2 + \text{XCH}_4$ mixture class at 50-atm fill pressure. The experimentally determined operational envelope for this mixture class is shown in Fig. 6.⁷ Note that in this mixture class, no "b" limit was observed; if

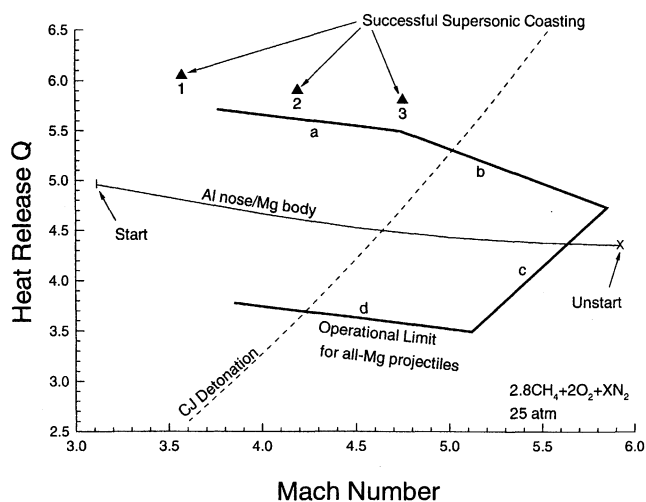


Fig. 5 Operational envelope (from Fig. 1) for magnesium projectiles in $2.8\text{CH}_4 + 2\text{O}_2 + \text{XN}_2$ at 25 atm, with results of combustion stripping experiments and Al nose-cone experiment.

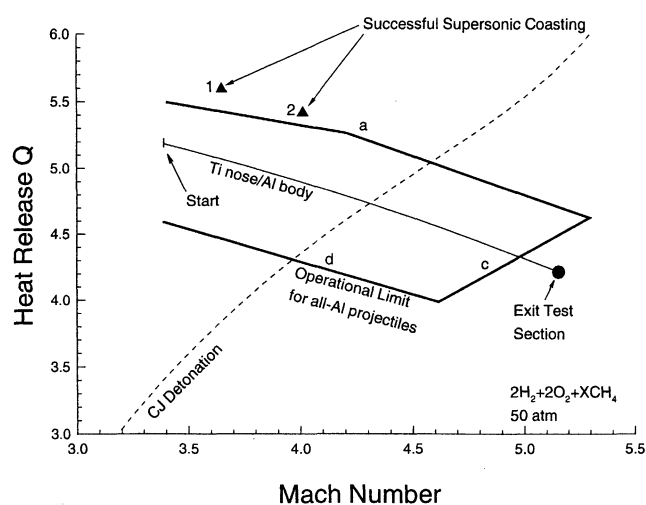


Fig. 6 Operational envelope of aluminum projectiles in $2\text{H}_2 + 2\text{O}_2 + \text{XCH}_4$ at 50 atm, with results of combustion stripping experiments and Ti nose-cone experiment.

ram acceleration was established, the projectile always accelerated to the transdetonative regime where it encountered the "c" limit. The maximum allowable heat release corresponded to a mixture of $2\text{H}_2 + 2\text{O}_2 + 5\text{CH}_4$, which forms the "a" limit in Fig. 6.⁷ Pressure traces for a projectile entering a more energetic mixture of $2\text{H}_2 + 2\text{O}_2 + 4.8\text{CH}_4$ at Mach 4 with the combustion wave still attached are shown in Fig. 7a. Upon entering the mixture from an intermediate stage of combustible gas, the projectile unstarted within 0.5 m. If the combustion wave is stripped with a stage of pure methane, however, the projectile is able to successfully coast more than 2 m with no noticeable change in wave activity at the projectile throat. In Fig. 7b the projectile transitioned from pure methane to the test mixture at Mach 3.6. No combustion activity was observed and the projectile proceeded down the tubes as if in a non-reacting gas. When the projectile Mach number was increased to Mach 3.9, a combustion wave was seen to develop in the wake and to eventually overtake the projectile, as seen in Fig. 7c. This result is almost identical to that observed in Fig. 4c. The results of these two combustion stripping experiments are labeled "1" and "2" and are compared to the envelope of ram accelerator operation with this class of mixtures in Fig. 6. Again, the ability of the projectile to successfully coast supersonically in mixtures substantially more energetic than those

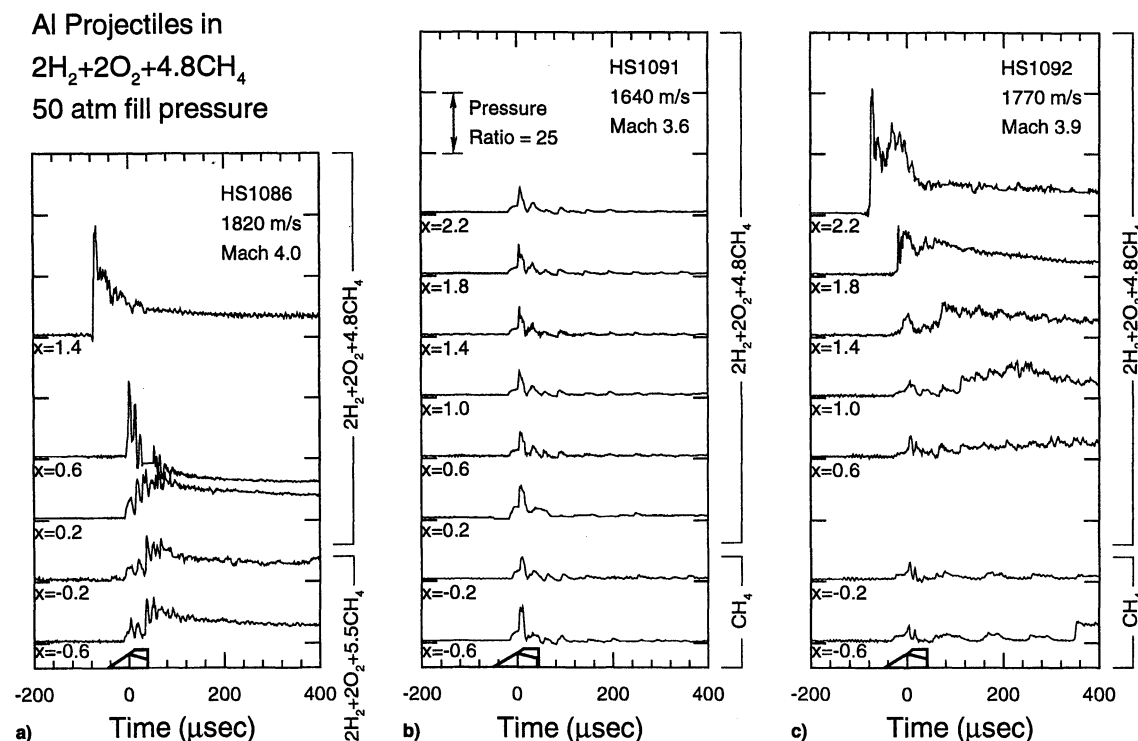


Fig. 7 Pressure traces from a mixture with a heat release value too great to support ram accelerator operation: a) projectile enters test mixture with combustion wave attached; b) projectile enters from inert stage without combustion wave attached; and c) projectile enters test mixture from inert stage at higher Mach number.

at the hot limit demonstrates that the unstart mechanism requires the presence of the combustion wave behind the projectile.

Material Effects

Most experiments performed to date at the UW ram accelerator facility have used projectiles fabricated from Mg and Al alloy. These materials are in many ways not suitable for the hypersonic environment to which they are subjected. They lose mechanical strength quickly with increasing temperature and have even been observed to burn in very high Mach number experiments.²⁰ Mg and Al continue to be used for their low cost, low density, and ease of machining. The use of these materials means that observed limits to operation are likely to be a result of a structural failure of the projectile and not gasdynamic or combustion phenomena. This section discusses experiments that investigated such material limits to ram accelerator operation.

Failure Mechanisms

The fact that the ram accelerator operates in a high-pressure (10–100 atm) environment and at Mach numbers approaching the hypersonic regime has raised concerns that the projectile is subjected to an intense heat flux. Several studies using numerical modeling indicated that Mg and Al projectiles are excessively heated after only a few milliseconds of operation at transdetonative and superdetonative velocities.^{21,22} Indeed, Naumann observed a correlation between unstarts and the time when the surface temperature of the nose cone and projectile fins is predicted to reach the point where ablation begins.²³ In addition, his calculations showed that during the brief time of an experiment the aerodynamic heating does not penetrate deep enough into the relatively thin-walled projectiles to compromise their mechanical strength.²³ Coupled CFD and structural modeling by Chew²⁴ predicted the nose tips are blunted in the time frame of these experiments, though this does not, by itself, cause an unstart. These same analyses indicate that Ti projectile components do not reach debilitating temperatures

in the experiments, implying that it could be a superior material for ram accelerator applications.^{24,25}

In addition to aerodynamic heat transfer to the nose cone, the projectile also suffers damage to the fins that are required to keep it centered in the tube. By observing asymmetries in the pressure distribution around the projectile, Hinkey et al.¹⁹ showed that Al projectiles in most ram accelerator experiments are canted by as much as 5°. Evidence of severe fin damage and removal has been observed in x-ray photographs taken of projectiles after being ram accelerated.^{26,27} Whether this fin deformation is the result of abrasion on the tube wall, melting, or shock-wave impingement is unknown, but the resultant projectile canting is obviously undesirable. CFD simulations of canted projectiles suggest that they may unstart under conditions in which a centered projectile would not.²⁸

Finally, magnesium and aluminum have the potential to react with oxygen in the propellant mixture.²⁹ Projectile burning has been observed in superdetonative ram accelerator experiments at Mach 6 and greater.^{20,26} Surface coatings of Al_2O_3 and ZrO_2 were shown to inhibit oxidation of projectile material, but these refractory coatings have problems remaining attached to the projectile.²⁶ At what velocity projectile burning becomes a factor is unknown.

The high speeds and short time scales of experiments and the destructive deceleration of projectiles after experiments makes assessing their condition prior to an unstart extremely difficult. Unstarts resulting from structural failure of the projectile cannot be distinguished from gasdynamic unstarts by pressure traces alone, such as those shown in Figs. 4a and 7a. A straightforward means of identifying material effects is to alter the material from which the projectile is fabricated. In this section suspected material limits to operation are investigated by altering projectile nose cones and bodies from Mg to Al and from Al to Ti.

Results

The c limit in Fig. 1 is not suspected of being the result of gasdynamic unstarts, but instead the result of a structural failure

of the Mg alloy (ZK60 AT5) four-fin projectiles used in these experiments. To verify this hypothesis, one of the experiments that comprises the *c* limit was repeated with an Al alloy (7075 T6) nose cone. The mixture used was $2.8\text{CH}_4 + 2\text{O}_2 + 5.7\text{N}_2$, which is the mixture used as a starter stage for all of the experiments reported in this paper. Because the starter and test stage are the same mixture in this case, the experiment consists of a single, 16-m-long stage. The resulting velocity–distance data are compared to the standard all-Mg projectile in Fig. 8. Note that the Al nose projectile was able to drive more than 3 m farther into the test section before unstart, reaching a final velocity of 2160 m/s, compared to 1990 m/s for the all-Mg projectile. The projectile masses are identical, so that the ability of the projectile to survive longer into the test section must be a result of material effects. Note that these tests were conducted at 30-atm fill pressure instead of 25-atm fill pressure to ensure that the eventual unstart would occur in the test section.

The result of this experiment with an Al nose cone is plotted with the experimentally determined envelope for Mg projectiles⁷ on the *Q*–*M* plane in Fig. 5. The fact that an Al nose-cone projectile can accelerate beyond the observed *c* limit shows this limit to be material dependent. The fact that the projectile eventually unstarted may have been a result of either the Al nose cone or the Mg body failing.

Also shown in Fig. 8 are results with Mg nose cones of different wall thicknesses but identical external geometries.³⁰ These experiments were motivated by the positive results obtained when Mg was replaced with Al. Perhaps, it was reasoned, the Al nose cone did not fail simply because it was stronger and did not crush or otherwise fail catastrophically. As the wall thickness of the Mg nose cone was increased from the nominal 2 mm thickness, however, the projectiles continued to unstart at the same velocity and within 1 m of the nominal experiment, even when a solid Mg nose cone was used. This result suggests that it is not the strength or internal structure that is the important factor, but rather the material at the projectile surface, particularly near the nose tip, which is responsible for the observed unstarts.

The observation that Al projectiles survive longer than Mg projectiles motivated their use in the investigation of the $2\text{H}_2 + 2\text{O}_2 + \text{XCH}_4$ class of propellant at 50 atm. Again, however, a suspected material limit was observed (labeled *c* in Fig. 6). To confirm a material effect, an experiment in a mixture ($2\text{H}_2 + 2\text{O}_2 + 6\text{CH}_4$) comprising the *c* limit was repeated using a Ti alloy (6Al-4V) nose cone. The results of this experiment, compared to the all-Al projectile (77 g), are shown in Fig. 9. Because of the high density of Ti, the projectile nose cone had a mass of 31 g, compared with the usual 24-g Al nose cone.

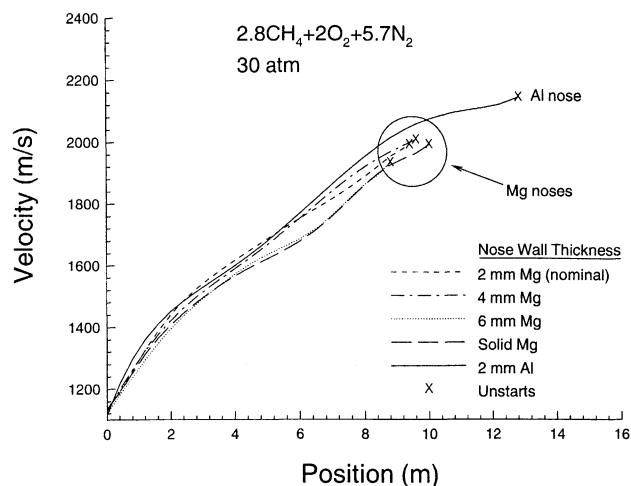


Fig. 8 Velocity–distance data for magnesium projectile with Al nose cone compared to standard, all-Mg projectiles with varying nose-cone wall thickness.

This increased mass is seen as slightly lower acceleration. The Ti nose projectile, however, was able to run farther into the test section; in fact, it exited the tube without unstart. The final velocity obtained was greater (2300 m/s compared with 2220 m/s), confirming that material effects are responsible for the observed *c* limit to operation of Al projectiles. The Ti nose experiment is compared with the operational envelope for Al projectiles in Fig. 6.

An interesting result of this experiment was that the projectile, upon reaching 2300 m/s, coasted at a nearly constant velocity for approximately 3 m before exiting the test section. This is not a termination of ram accelerator drive, because a projectile coasting through a nonreactive mixture for this distance would lose significant velocity because of drag. The pressure traces also show that the driving combustion wave was still attached. Instead, it is postulated that the projectile reached a thrust-equals-drag condition and was operating in a steady-state manner. This possibility is discussed further in Ref. 20.

The increase in limiting velocity observed with different nose-cone materials motivated an investigation of the effectiveness of using Ti projectile components. These experiments were conducted in a single stage of 50-atm propellant mixture consisting of $3\text{CH}_4 + 2\text{O}_2 + 5.7\text{N}_2$ with an entrance velocity of 1140 m/s. The velocity–distance data for the Ti series of experiments are shown in Fig. 10. The Al-nose/Al-body combination (76.9 g), used as the control experiment, unstarted at 2070 m/s after accelerating for 7.2 m. The Ti-nose/Al-body

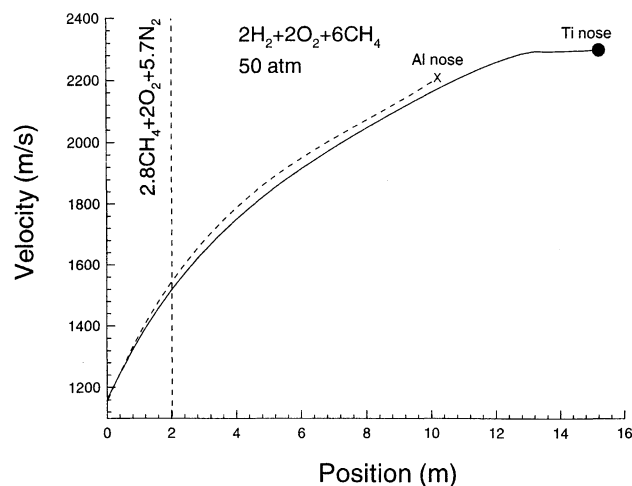


Fig. 9 Velocity–distance data for aluminum projectile with Ti nose cone compared to standard, all-Al projectile.

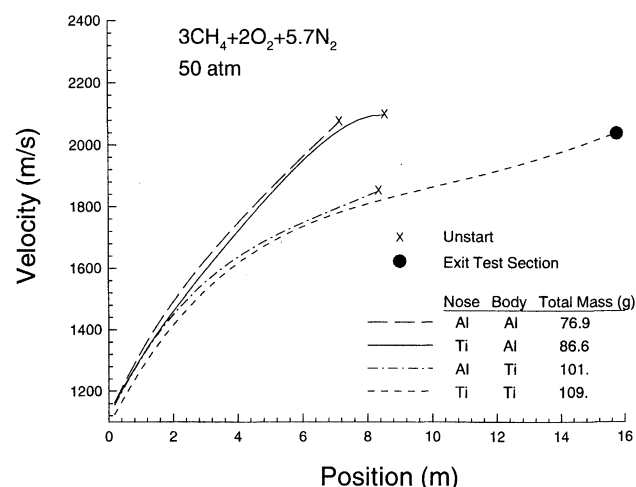


Fig. 10 Velocity–distance data for projectiles with different combinations of Al and Ti nose cones and bodies.

combination (86.6 g) reached 2100 m/s in 8.5 m before unstarting; however, it appeared to be coasting at a nearly constant velocity for the last 1.5 m of its run. This may be akin to the coasting observed at 2300 m/s in the methane diluted mixture (Fig. 9). The Ti body with an Al nose traveled just as far into the test section as the prior two projectiles, but it had only reached 1850 m/s at this point because of its increased mass. The all-Ti projectile accelerated through the entire test section without unstart and exited the tube at 2050 m/s.

Discussion

The ability of the projectile, if stripped of the combustion wave, to supersonically coast in a mixture in which it would otherwise immediately unstart is strong evidence that the unstart is caused by a surge of the combustion wave past the projectile throat. This result suggests that if the projectile geometry were modified to better contain the driving combustion wave, operation in more energetic mixtures might be realized. The unstart mechanism is obviously not a consequence of pre-ignition or detonation of the combustible gas flowing past the projectile forebody.

The ability of the combustion wave to reignite in the wake of the projectile is also intriguing. This phenomenon was only observed when the projectile was above Mach 3.6. At lower Mach numbers, no combustion activity was seen. The higher shock and stagnation temperatures resulting from higher Mach numbers are apparently required to reignite the combustion wave behind the projectile. This may explain why wave fall-offs are almost never observed while a projectile is accelerating: as the projectile reaches higher Mach numbers, the increasing shock and stagnation temperatures promote a more rapid combustion process, and so the projectile cannot outrun the combustion wave. Reignition in the wake of a coasting projectile also suggests that interaction with the obturator may not be required to initiate thermally choked operation. Indeed, ram acceleration has been re-established by injecting the projectile from inert gas into a mixture less energetic than that shown in Fig. 4.³¹

The exact mechanism by which the combustion wave is forced past the projectile throat is unclear. CFD calculations suggest that coupled boundary-layer combustion and an oblique shock system move up the body.^{13,14} Expansion tube experiments with stationary models have shown that combustion can couple with the boundary layer to force a separation shock upstream.³² Other examples of boundary-layer combustion forcing a separation shock upon a projectile can be seen in firings of conical projectiles with boattail afterbodies into combustible gases.³³

Turning to material effects, the suspicion that the *c* limit in Fig. 5 is a material effect was confirmed by repeating an experiment with an Al nose cone, which allowed it to reach a higher velocity before unstart. A similar change from an Al to a Ti nose cone proved a material effect in the *c* limit of Fig. 6 as well. In that experiment, the use of a Ti nose cone completely eliminated the unstart. The fact that a solid Mg nose cone failed at a lower velocity and earlier in the tube than a thin-walled Al nose cone suggests that the surface material characteristics are more important than the overall structural integrity of the nose cone. This concurs with the computational studies of Chew,²⁴ which show that the nose tip will quickly ablate while the rest of the nose cone remains intact.

Examining the effect of replacing different projectile components with Ti suggested that the nose cone is the more critical component, because the Al-nose/Ti-body projectile in Fig. 10 unstarted at a velocity even lower than the all-Al projectile. Failure of the body, however, was suspected in the unstart of the Ti-nose/Al-body projectile. Only the all-Ti projectile exited the test section without unstart. The ability of the Ti projectile to traverse the entire 16-m-long test section suggests that this material can withstand greater heat transfer than Al. Heat flux to a vehicle in the hypersonic regime is usually assumed to

vary with the cube of velocity.³⁴ If the cube of the observed velocity as a function of time is integrated from the entrance to the time of unstart or exiting the test section, the result shows that the all-Ti projectile in Fig. 10 withstood more than twice the integrated heat transfer of aluminum or combination Ti/Al projectiles without failing. Thus, Ti may have the durability to enable investigating the true gasdynamic limits of the ram accelerator.

The positive identification of both material and gasdynamic limits to ram accelerator operation answers an important question: What mechanism limits the maximum velocity of a particular projectile in a given mixture class? From Fig. 1, the answer is seen to be *both* gasdynamic and structural mechanisms. The maximum velocity obtained in the $2.8\text{CH}_4 + 2\text{O}_2 + \text{XN}_2$ class of propellant occurs where the gasdynamic limit *b* and the material limit *c* intersect. If an experiment is terminated with a gasdynamic unstart as the result of too energetic a mixture, a greater velocity can be obtained with a cooler mixture by increasing the dilution, even though the projectile experiences a lower average acceleration. If an experiment results in a structural failure, increasing the mixture heat release will result in an unstart earlier in the test section, but the unstart will be at a greater velocity. The same is true of the $2\text{H}_2 + 2\text{O}_2 + \text{XCH}_4$ class of propellant in Fig. 6.⁷

The fact that the gasdynamic (*a* and *b*) and material (*c*) limits in Figs. 5 and 6 have different signs to their slopes also implies a means to diagnose unstarts without resorting to a change in projectile material. If increasing the mixture heat release results in a greater unstart velocity in a shorter distance of travel, the unstart mechanism is structural. If increasing the mixture heat release causes a reduction in unstart velocity, the mechanism is gasdynamic.

The possibility of a combined gasdynamic and structural unstart mechanism also exists, such as projectile canting that allows the combustion wave to more easily be disgorged past the projectile throat.^{19,28} The fact that the material limits are parallel to the CJ relation in the *Q-M* plane and the possibility of a thrust-equals-drag condition at some fraction above the CJ speed also suggests a gasdynamic and material coupling, i.e., a gasdynamic limit on positive thrust that increases the projectile dwell time at that velocity, eventually causing a structural failure.²⁰

Conclusions

By stripping the combustion wave from the projectile with a stage of inert gas and then injecting it back into a combustible mixture, the ability of a projectile to coast supersonically without unstart in a combustible mixture that does not support ram acceleration has been demonstrated. This result proves that the gasdynamic unstart mechanism in mixtures that are too energetic is a surge of the combustion wave over the projectile. The unstart is not the result of precombustion or detonation initiation in the supersonic flow over the projectile's nose cone.

Unstarts that occur in experiments with cooler mixtures that allow the projectile to accelerate for long distances have been shown to be caused by structural failure of the projectile. By changing the projectile material to a more refractory metal, the maximum Mach number of operation can be increased. The projectile nose cone, which is exposed to intense heat transfer, appears to be the more critical component. To date, only an all-Ti projectile has demonstrated the ability to survive in the most adverse environments experienced in these experiments.

Acknowledgments

This work was supported in part by Army Research Office Grant DAAL03-92-G-0110 and U.S. Air Force Office of Scientific Research Grant F49620-92-J-0375. The assistance of Akihiro Sasoh and Thomas Imrich with the laboratory experiments is greatly appreciated. Malcolm Saynor machined the

magnesium projectiles. 4-D Manufacturing Inc. of Redmond, WA fabricated the aluminum and titanium projectiles.

References

- ¹Hertzberg, A., Bruckner, A. P., and Bogdanoff, D. W., "Ram Accelerator: A New Chemical Method for Accelerating Projectiles to Ultrahigh Velocities," *AIAA Journal*, Vol. 26, No. 2, 1988, pp. 195–203.
- ²Hertzberg, A., Bruckner, A. P., and Knowlen, C., "Experimental Investigation of Ram Accelerator Propulsion Modes," *Shock Waves*, Vol. 1, No. 1, 1991, pp. 17–25.
- ³Higgins, A. J., Knowlen, C., and Bruckner, A. P., "An Investigation of Ram Accelerator Gas Dynamic Limits," AIAA Paper 93-2181, June 1993.
- ⁴Higgins, A. J., "Gas Dynamic Limits of the Ram Accelerator," M.S. Thesis, Univ. of Washington, Seattle, WA, 1993.
- ⁵Knowlen, C., Higgins, A. J., and Bruckner, A. P., "Investigation of Operational Limits to the Ram Accelerator," AIAA Paper 94-2967, June 1994.
- ⁶Knowlen, C., Higgins, A. J., and Bruckner, A. P., "Aerothermodynamics of the Ram Accelerator," AIAA Paper 95-0289, Jan. 1995.
- ⁷Higgins, A. J., Knowlen, C., and Bruckner, A. P., "Ram Accelerator Operating Limits, Part 1: Identification of Limits," *Journal of Propulsion and Power*, Vol. 14, No. 6, 1998, pp. 951–958.
- ⁸Ghorbanian, K., Pratt, D. T., and Humphrey, J. W., "Supersonic Flow of Reactive Gases over Sphere-Cone Bodies," AIAA Paper 92-0091, Jan. 1992.
- ⁹Lefebvre, M. H., and Fujiwara, T., "Numerical Modeling of Combustion Processes Induced by a Supersonic Conical Blunt Body," *Combustion and Flame*, Vol. 100, No. 1, 1995, pp. 85–93.
- ¹⁰Leblanc, J. E., Lefebvre, M. H., and Fujiwara, T., "Detailed Flowfields of a RAMAC Device in H₂-O₂ Full Chemistry," *Shock Waves*, Vol. 6, No. 2, 1996, pp. 85–92.
- ¹¹Ghorbanian, K., and Sterling, J., "Gas Dynamic Unstart in Supersonic Ram Accelerators," AIAA Paper 96-2948, July 1996.
- ¹²Messersmith, N. L., and Reeb, A. B., "Analysis of Ram Projectile Acceleration and Unstart Using Oblique Detonation Theory," AIAA Paper 96-2947, July 1996.
- ¹³Soetrisno, M., Imlay, S. T., and Roberts, D. W., "Numerical Simulations of the Transdetonative Ram Accelerator Combusting Flow Field on a Parallel Computer," AIAA Paper 92-3249, July 1992.
- ¹⁴Yungster, S., "Navier-Stokes Simulation of Supersonic Combustion Flowfield in a Ram Accelerator," AIAA Paper 91-1916, June 1991.
- ¹⁵Nusca, M. J., "Reacting Flow Simulation for a Large Scale Ram Accelerator," AIAA Paper 94-2963, June 1994.
- ¹⁶Burnham, E. A., Hinkey, J. B., and Bruckner, A. P., "Investigation of Starting Transients in the Thermally Choked Ram Accelerator," 29th JANNAF Combustion Subcommittee Meeting, NASA Langley Research Center, Hampton, VA, Oct. 1992.
- ¹⁷Burnham, E. A., "Investigation of Starting and Ignition Transients in the Thermally Choked Ram Accelerator," Ph.D. Dissertation, Univ. of Washington, Seattle, WA, 1993.
- ¹⁸Bruckner, A. P., Knowlen, C., Hertzberg, A., and Bogdanoff, D. W., "Operational Characteristics of the Thermally Choked Ram Accelerator," *Journal of Propulsion and Power*, Vol. 7, No. 5, 1991, pp. 828–836.
- ¹⁹Hinkey, J. B., Burnham, E. A., and Bruckner, A. P., "Investigation of Ram Accelerator Flow Fields Induced by Canted Projectiles," AIAA Paper 93-2186, June 1993.
- ²⁰Knowlen, C., Higgins, A. J., Bruckner, A. P., and Bauer, P., "Ram Accelerator Operation in the Superdetonative Velocity Regime," AIAA Paper 96-0098, Jan. 1996.
- ²¹Seiler, F., and Naumann, K. W., "Bow Shock Wave Heating and Ablation of a Sharp-Nosed Projectile Flying inside a Ram Accelerator," *Proceedings of the 19th International Symposium on Shock Waves*, edited by R. Brun and L. Z. Dumitrescu, Springer-Verlag, Berlin, 1995, pp. 183–188.
- ²²Chew, G., and Bruckner, A. P., "A Computational Study of Projectile Nose Heating in the Ram Accelerator," AIAA 94-2964, June 1994.
- ²³Naumann, K. W., "Heating and Ablation of Projectiles During Acceleration in a Ram Accelerator Tube," AIAA Paper 93-2184, June 1993.
- ²⁴Chew, G., "Projectile Nose Heating in the Ram Accelerator," Ph.D. Dissertation, Univ. of Washington, Seattle, WA, 1995.
- ²⁵Seiler, F., and Mathieu, G., "Boundary Layer Model for Calculating the Heat Transfer into a Ram Projectile Fired in a Ram Accelerator," *Proceedings of the 2nd International Workshop on Ram Accelerators*, Univ. of Washington, Seattle, WA, 1995.
- ²⁶Patz, G., Seiler, G., Smeets, G., and Srulijes, J., "Status of ISL's RAMAC 30 with Fin Guided Projectiles Accelerated in a Smooth Bore," *Proceedings of the 2nd International Workshop on Ram Accelerators*, Univ. of Washington, Seattle, WA, 1995.
- ²⁷Giraud, M., Legendre, J. F., Simon, G., Henner, M., and Voisin, D., "RAMAC in 90 mm Caliber or RAMAC 90: Starting Process, Control of the Ignition Location, and Performance in the Thermally Choked Propulsion Mode," *Proceedings of the 2nd International Workshop on Ram Accelerators*, Univ. of Washington, Seattle, WA, 1995.
- ²⁸Soetrisno, M., Imlay, S. T., and Roberts, D. W., "Numerical Simulations of the Superdetonative Ram Accelerator Combusting Flow Field," AIAA Paper 93-2185, June 1993.
- ²⁹Liberatore, F., "The Effects of Real Material Behavior on Ram Accelerator Performance," *Proceedings of the 2nd International Workshop on Ram Accelerators*, Univ. of Washington, Seattle, WA, 1995.
- ³⁰Imrich, T. S., "The Impact of Projectile Geometry on Ram Accelerator Performance," M.S. Thesis, Univ. of Washington, Seattle, WA, 1995.
- ³¹Higgins, A. J., "The Effect of Confinement on Detonation Initiation by Blunt Projectiles," AIAA Paper 97-3179, July 1997.
- ³²Srulijes, J., Smeets, G., and Seiler, F., "Expansion Tube Experiments for the Investigation of Ram-Accelerator-Related Combustion and Gasdynamic Problems," AIAA Paper 92-3246, July 1992.
- ³³Behrens, H., Lehr, H., Struth, W., and Wecken, F., "Shock-Induced Combustion by High-Speed Shots in Explosive Gas Mixtures," French-German Research Inst. of Saint-Louis (ISL), Rept. 4/67, 1967.
- ³⁴Anderson, J. D., *Hypersonic and High Temperature Gas Dynamics*, McGraw-Hill, New York, 1989, p. 289.